Article

Combining living microorganisms with regenerated silk provides nanofibril based thin films with heat responsive wrinkled states for smart food packaging

Luca Valentini[1,*], Silvia Bittolo Bon[1] and Nicola Pugno[2,3,4*]

[1] Dipartimento di Ingegneria Civile e Ambientale, Università di Perugia, UdR INSTM, Strada di Pentima 4, 05100 Terni - Italy. E-mail: luca.valentini@unipg.it

[2] Laboratory of Bio-Inspired and Graphene Nanomechanics, Department of Civil, Environmental and Mechanical Engineering, University of Trento, Trento, Italy. E-mail: nicola.pugno@unitn.it

[3] School of Engineering and Materials Science, Queen Mary University of London, Mile End Road, London, United Kingdom

[4] Ket-Lab, Edoardo Amaldi Foundation, Italian Space Agency, via del Politecnico snc, I-00133 Roma, Italy

* Correspondence: luca.valentini@unipg.it; Tel.: +39-0744-492924; nicola.pugno@unitn.it; Tel.: +39-0461-282525

Abstract: Regenerated silk (RS) is a protein-based "biopolymer" that enables the design of new materials; here we sought to "bionic" the process of regenerated silk production by fermentation assisted method. Based on yeast's fermentation, here we produced a living hybrid composite made of regenerated silk nanofibrils and a single-cell fungi, the *Saccharomyces Cerevisiae* yeast extract, by fermentation of such microorganisms at room temperature in the dissolution bath of silkworm silk fibers. The fermentation-based processing enhances the beta-sheet content of the RS, corresponding to a reduction in water permeability and CO_2 diffusion through RS/yeast thin films enabling the fabrication of mechanically robust film that enhances the food storage durability. Finally a transfer print method, which consists of transferring RS and RS/yeast film layers onto self-adherent paraffin substrate, was used for the realization of heat – responsive wrinkles by exploiting the high thermal expansion of the paraffin substrate that regulates the applied strain, resulting in a switchable coating morphology from the wrinkle-free state to a wrinkled state if the food temperature overcomes a designed threshold. We envision that such efficient and smart coatings can be applied for the realization of smart packaging that through such temperature sensing mechanism can be used to control the food storage conditions.

Keywords: bionic composites; thin films; mechanical properties.

---

1. Introduction

Living microorganisms have long been used in food preservation [1,2]; such microorganisms form living surfaces that provide an attractive platform to the development of functional materials. At present, biotech companies uses fungi to produce valuable products [3], thus combining the fermentation mechanism of some microorganisms with biomaterials could give a raise to bionic composites with novel properties.

Between such novel products, innovative packaging solutions to increase the shelf-life of fresh fruits by slowing down their metabolism so they remain fresh and appetizing for longer and the development of sensors to monitor if perishable food in the cold chain is maintained in the desired temperature range to prevent the growth of pathogens and spoilage microorganisms, are still challenging.

Concerning the sensing issue, spontaneous generation of wrinkles induced by the buckling of a thin skin due to thermal contraction of the underlying substrate may be used as diffraction gratings in optical sensors, and as the basis for monitoring temperature changes in food cold chain. In this regard, micro/nanoscale surface patterns obtained by coupling a stiff skin to a soft substrate have been used to create reversible patterns that are responsive to temperature and provided unique surface morphology to sense temperature changes [4-7].

From the material point of view, silk fibroin is an ideal candidate for the packaging applications since it is a biocompatible structural protein that can processed to obtain films which recently have been used as biodegradable and edible sensors to monitor food degradation [8-10]. The polymorphism of silk fibroin (i.e. random coil, silk I, and silk II structures) can be also tailored by controlling the content of β-sheet crystals that enables the correct gas exchange and water vapour permeability through silk-based membranes [11-13]. Between the different fabrication methods, transfer printing is the most known method for interfacing silk on soft substrates [14]. In this regard, the hidden strength and stiffness of natural honeycomb walls constructed from recycled silk and wax secreted by worker bees [15-17] is reminiscent of modern fiber-reinforced composite laminates.

Taking inspiration from the honeybee comb cell wall, a self-adhesive and soft thermoplastic paraffin wax, can be used to stick RS film to produce a bilayer system [18]. Being the paraffin wax a material with high thermal expansion coefficient, wrinkles occur to minimize the total energy of such bilayer system when the compressive strain, caused by the thermal expansion coefficients and rigidities mismatches between the skin layer and the substrate induced by thermal stimulus.

Inspired by our previous work [19] on the production of beer's yeast cells/carbon nanotube composite directly by fermentation of the yeast extract in presence of carbon nanotube aqueous dispersion, we therefore designed a robust composite coating combining inert (RS) and living parts (brewer's yeast). It was observed that once *Saccharomyces Cerevisiae* yeast cells were fermented by nutrient addition into a silk fibroin solution, the regenerated silk shows a higher content of beta-sheet structures. Moreover, the microorganism growth increased the cell density and reduced the porosity of the RS membrane limiting the exchange of water and gas diffusion. As conceptual proof, we demonstrated as an example that the deposition of such living coating on fruits helps the preservation of their shelf-life. Finally, we demonstrate that RS based film layers can be laminated onto a paraffin wax substrate for the realization of temperature – responsive bilayer systems.

2. Materials and Methods

For the preparation of RS film, commercial *B. mori* silk cocoons were boiled for 1 h in distillated water solution of 0.025 wt % $NaHCO_3$, rinsing with distilled water every 30 min. to remove the sericin. According to the method adopted by Kaplan et al. [20], the degummed silk (i.e. 0.2 g) was then added to a $CaCl_2$ (i.e. 0.14 g) - formic acid (i.e. 20 ml) solution and stirred over the night at 40°C yielding an 1 wt % solution. Water solution (50 mg/ml) of *Saccharomyces Cerevisiae* based commercial beer yeast extract was prepared separately by mechanical stirring at 30 °C for 1 h. After that, sucrose was added to start the fermentation. The amount of sugar added is usually between 3 and 5 times the weight of the medium. Water solution of fermenting yeast was then added to the silk fibroin solution. RS/yeast films were prepared by leaving the silk-yeast solution to evaporate for 12 h in a polystyrene Petri dish (diameter 15 cm). The growth of yeast cells was monitored by the optical density (OD) method, measuring the absorbance at wavelength 600 nm and temperature 30°C of the yeast and RS/yeast solutions in sucrose growth medium. The morphology of the films was investigated by optical and field emission scanning electron microscopy (FESEM). Fourier transform infrared (FTIR) analysis was performed in a Jasco FTIR FT/IR-615 spectrometer, equipped with an ATR mode in the wave number range from 400 to 4000 cm^{-1}. X-ray diffraction was performed using a Bruker D8 Advance diffractometer with a radiation source of CuKα and wavelength λ=0.154 nm operated at 40 kV and 40 mA. The incidence angle (2θ) was varied between 2° and 60° and the scan rate was 0.02°/s. The tensile properties of films were measured using a universal tensile testing machine (Lloyd Instr. LR30K) with a 50 N static load cell. The film samples were cut into strips (30 mm × 12 mm). The gauge length was 20 mm, and the extension rate was set at 2 mm/min.

 doi:10.20944/preprints201806.0320.v1

The effect of different types of coatings on bananas freshness was evaluated by monitoring the colour change through time-lapse photography. The water permeability was determined after soaking a sponge in water and subsequently dip coating the sponge in RS and RS/yeast solutions. The variation of the weight was monitored at different hours with a standard laboratory balance (Mettler Toledo AB135-S/FACT). The weight variation was calculated as an average of three measurements for each coating. The respiration rate of bananas was evaluated by monitoring the CO_2 production. In brief, bananas were placed in a sealed FTIR chamber and the production of CO_2 was monitored by measuring the evolution of the CO_2 absorption peak over period of 7 days (see supplementary material Fig. S1). This measurement takes into account the initial background performed in air to remove the initial contribution of the carbon dioxide moisture of the air.

For the adopted transfer print process to realize the bilayer system, regenerated silk was transferred to Parafilm film (Parafilm M®, Pechiney Plastic Packaging Company) through direct transfer process, which consists of placing RS and RS/yeast free standing films on the receiving Parafilm substrate while applying with a hot press a pressure of 2kPa at 60°C for 15 min.; the composite material separates spontaneously from the press plates as it cools. The obtained bilayer systems were heated at 60°C and cooled to room temperature (i.e. $\Delta T \approx 40$°C) and AFM was carried out to measure wrinkle morphology in tapping mode (easyScan DFM system).

3. Results and discussion

The production method adopted for the realization of thin films with the aid of living microorganisms is schematically reported in Fig. 1a. The yeast fermentation was implemented into a $CaCl_2$-formic acid dissolution system, which can be used to produce large films (Fig. 1b) with a nano-fibrillar structure (Fig. 1c).

Changes in structure of the films deposited after the fermentation assisted silk dissolution were detected by FTIR and X Ray Diffraction (XRD). The β-sheet (crystalline) content was determined by the deconvolution of the amide I region (1580 - 1720 cm^{-1}) estimating the ratio between the peak area in the wavenumber region of 1622~1637 cm^{-1}, which is the main absorbance region of β-sheet crystal in amide I [21], and the whole area of the amide I comprising the peaks of the structural components including turns (T) and random coil (R). The deconvolution of the amide I band provides an estimation of β-sheet structure in the RS and RS/yeast of 37% and 44%, respectively (Figs. 1d-e).

The XRD data in Fig. 1f show the RS/yeast film is characterized by diffraction peaks at 2Θ values of 20.4° and 25.4°, corresponding to silk I structure [22,23]. RS film also showed silk I and silk II crystal structures, having diffraction peaks at 20.4° and 29.0°. Compared with RS/yeast, the silk I peak at 25.0° disappeared, indicating more silk II formation.

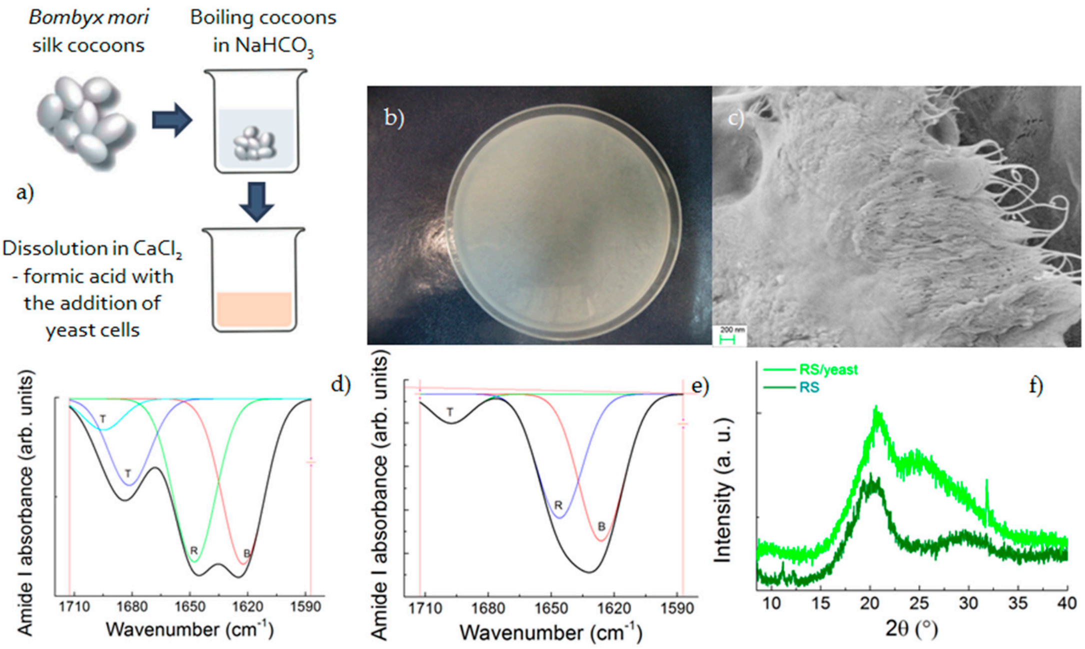

Figure 1. (a) Scheme of silk fibroin production using regenerated silk. (b) Visual appearance of the RS/yeast film and (c) FESEM image of silk nanofibrils. (d-e) FTIR spectra of regenerated silk and RS/yeast films, respectively. The coloured lines represent the components of the amide I band and are indicated as β-sheets (B), random coil (R) and turns (T). (f) XRD results of regenerated silk and RS/yeast films.

The cell division of yeast occurs by budding in which a daughter is initiated from the mother cell, followed by nuclear division and finally cell separation. The yeast cell growth reported in Fig. 2 shows the three main phases: the lag phase where the individual cells are activated in preparation for division, the exponential phase once the cell starts actively metabolizing shortly after the cells divide and finally the stationary phase when metabolism slows and the cells stop rapid cell division [24]. The factors that cause cells to enter stationary phase are related to change in the environment typically caused by high cell density. The data reported in Fig. 2a state the stability of the yeast cells to proliferate also with the presence of formic acid in the nutrient broth. The effects of RS addition during the growth curve are demonstrated in Fig. 2a by measuring the OD during the cell growth. The OD curve of the yeast cells is substantially altered by the RS addition, with the effect on the lag time and final cell yield being particularly pronounced: RS/yeast cells have a lag phase of ~ 2-3 hrs, after which they proliferate rapidly, in comparison, the neat yeast cells show an increased lag phase of ~ 10 hrs. The morphology of the stationary phase for the RS/yeast system observed by means of FESEM and optical microscopy (Figs. 2b-c) indicates the cell proliferation for such culture.

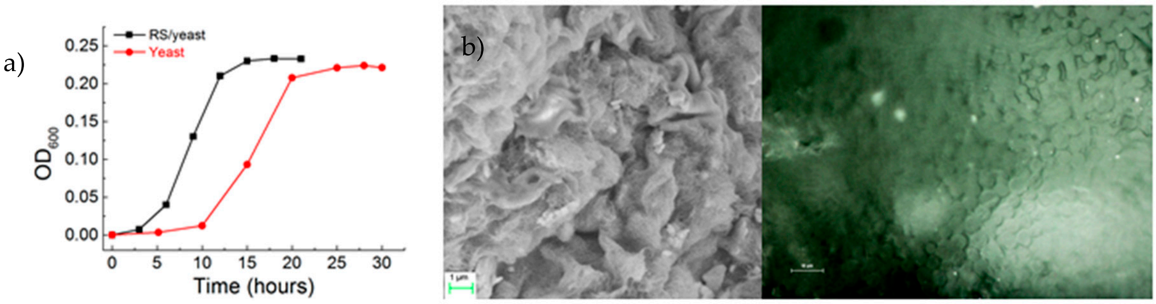

Figure 2. (a) OD measured at 600 nm wavelength during growth of neat *Saccharomyces Cerevisiae* and *Saccharomyces Cerevisiae* in RS with sucrose until stationary was reached. (b) Appearance under FESEM and optical microscope of the RS/yeast cell growth during the stationary phase.

In order to demonstrate potential application of such living coating in consumer exposed food the mechanical robustness of the films is required to withstand, for example, handling procedures. Figure 3a represents typical stress/strain curves obtained from testing of yeast, RS and RS/yeast samples. The maximum average toughness (i.e. the area underlying the stress-strain curves) obtained from RS/yeast sample was 0.14 MPa (Fig. 3b) as well as the highest average strength (i.e. the stress at the ultimate strain) obtained was 1.26 MPa, with a maximum elastic modulus of 37.2 MPa recorded. The improved mechanical properties with fermentation-based dissolution of silkworm silk fibers agree with our previous studies reported for the assisted-fermentation synthesis of bionic composites [19,25]. In these studies, addition of carbon nanotubes (CNTs) and/or graphene in the fermentation broth, resulted in composites with higher toughness value. In our studies, tensile tests on dried composite films were rationalized in terms of a CNT cell bridging mechanism where the strongly enhanced strength of the composite is governed by the adhesion energy between the bridging CNTs and the matrix. The presence of glucose can plasticize regenerated silks and increase the ultimate strain leading to toughness values (see Table 1) that are comparable to those measured for traditional biopolymers used for food packaging [26,27] being in our case as added value the edibility of the coating.

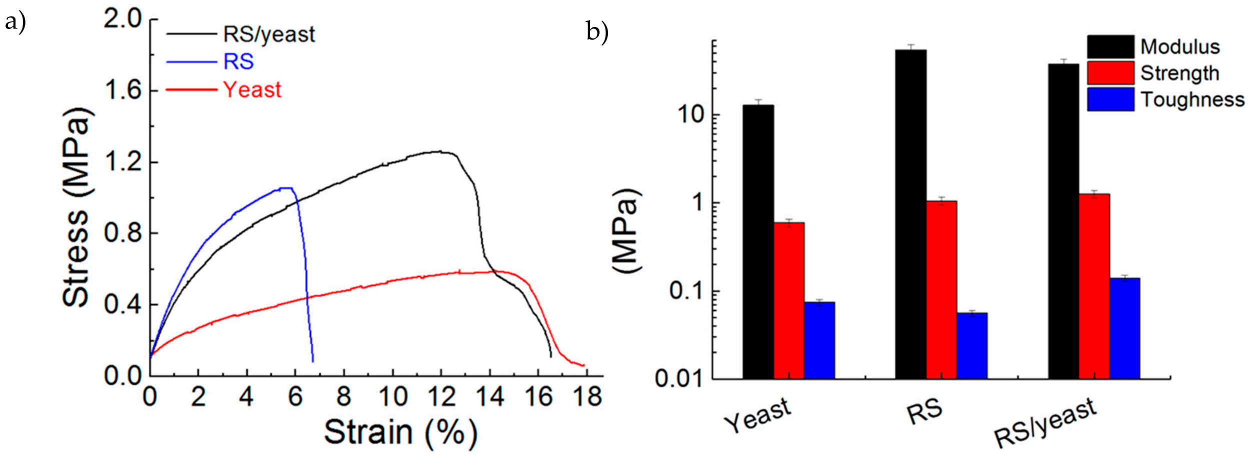

Figure 3. (a) Stress-strain curves from testing of yeast, RS and RS/yeast samples. The curves represent analysis performed on three different samples. (b) Effect of yeast fermentation on modulus, strength, and toughness of RS film. The modulus, strength, and toughness of neat yeast film have been reported for comparative purposes.

Table 1. Mechanical properties of various biopolymers for food packaging [27]. σ* — specific tensile strength, E* — specific tensile modulus, ε — ultimate strain.

Type of biopolymer	Toughness (MPa)	σ* (Nm/g)	E* (kNm/g)	ε (%)
RS/yeast (this work)	0.14	1.1	0.032	15.4
PLA	0.26	16.8	0.3	2.5
PLLA	0.23	40.0	2.2	3.0
PDLLA	0.28	22.1	0.8	2.0
PDLLA/PGA50/50	0.41	30.9	0.8	2.0

In general, coatings for food packaging beyond the mechanical robustness should exert low permeability to water vapors; fruit dehydration is, in general, an indicator of the breakdown of the protective skin, which results in loss of turgor and water evaporation. We observe that the increase in beta-sheet content yields a less water permeability through the RS/yeast membrane as indicated by the less variation of the initial weight of soaked sponges coated with different types of coatings, as reported in Fig. 4a (see supplementary material Fig. S2). These results are in agreement with those obtained by Omenetto et al.10 who showed that when the silk fibroin beta-sheet content is in the range of 36%–58%, the water vapour permeability is five times smaller than that measured for the film with a lower beta-sheet content.

Many fresh fruits have high metabolic activity and due to microbial attack they result in short conservation time, colour change (Fig. 4b), and off-flavour. The change in colour of fresh fruit, in particular, is associated to ethylene production and cell respiration. To evaluate the exploitation of RS/yeast film as barrier coating, the change in color of coated and non-coated fresh bananas was evaluated (Fig. 4b). Time-lapse photography shows that RS/yeast coating decreases the fruit degradation, when compared to uncoated or RS coated fruit at day 7. During the continuing metabolism of the fresh fruit, oxygen is transformed into carbon dioxide; thus gas permeation through a coating film plays a crucial role in fruit storage. To prevent the spoilage of fresh fruits it is necessary to reduce the breathing process. In our case, the higher beta-sheet content of the RS/yeast film decreases the production of CO_2, which indicated a decrease in the respiration rate of the fruits (Fig. 4c).

 doi:10.20944/preprints201806.0320.v1

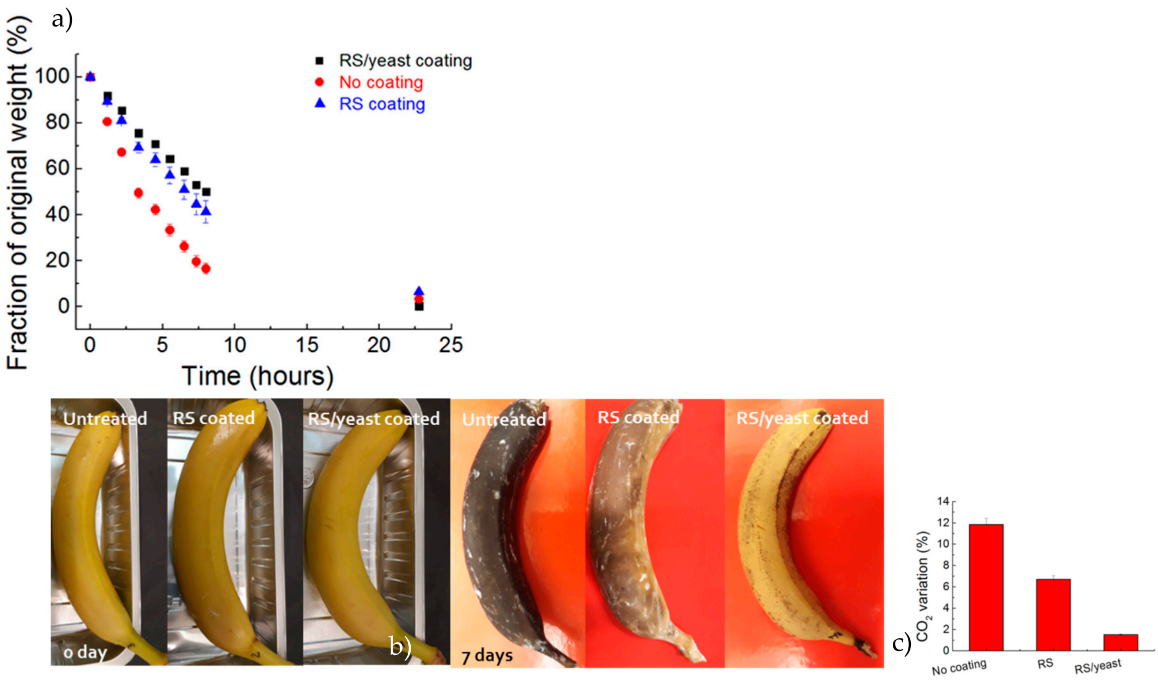

Figure 4. (a) Weight loss of sponges soaked in water and stored for up to 25 hours at 23 °C and 32% RH. Sponges were stored without coating or after dip coating with RS and RS/yeast suspensions, respectively. (b) Evaluation of bananas degradation. Fruits were stored at 23 °C and 32% RH as received and after coating with silk/yeast film. Time lapse photography of banana degradation, indicating that silk/yeast coating reduces the degradation rate. (c) CO_2 variation of uncoated, RS coated and RS/yeast coated bananas, respectively.

Another very interesting property of such silk nanofibrils relies on their ability to self-assemble giving rise to sol-gel transition with rapid gelation time induced by the presence of salts [28,29]. Pregelation occurs when a fresh solution has a β-sheet content of about 20% with negligible intermolecular bindings; gelation is then induced by interchain interactions that become irreversible with the formation of β-sheet intermolecular structures of the gel phase [29]. In our case, the gelation was observed when KNO_3 salt was added to silk nanofibrils/yeast/formic acid solution (Figure 5). Without salt, the RS/yeast retains with time a sol characteristic (Fig. 5a). In comparison with the sol RS/yeast solution, the RS/yeast with salt transform into a semi-solid gel within several hours, together with the appearance of a strong infrared absorption peak at 1626 cm^{-1} due to the formation of strong β-sheet strctures (Fig. 5b).

Preprints (www.preprints.org) | NOT PEER-REVIEWED | Posted: 20 June 2018 doi:10.20944/preprints201806.0320.v1

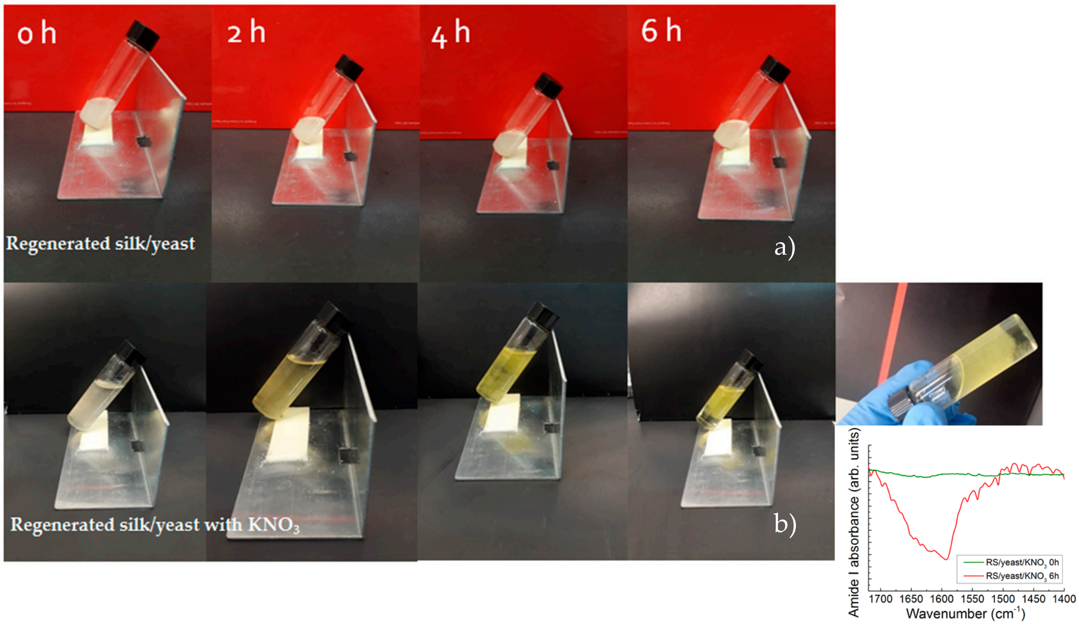

Figure 5. Dynamic optical morphology of the (a) RS/yeast and (b) RS/yeast/KNO_3 solutions resulting at different times (temperature 37°C). The inset of panel (b) shows the evolution of the amide I FTIR band of the RS/yeast/KNO_3 solution with time and gelation of the RS/yeast/KNO_3 solution.

Considering the application of controlling the food cold chain, it is essential to design a bilayer packaging system where the mechanical properties of the top skin layer when laminated onto a soft substrate will be beneficial for the creation of temperature-driven surface patterning. Figure 6a shows the RS and RS/yeast films laminated onto the paraffin wax substrate. Wrinkle formation is typically connected to the high thermal expansion coefficient of the substrate used for the transfer. Parafilm is worldwide used in research laboratories as self-adhesive and sealant plastic foil, it is soft (tensile strength ≈2.0MPa) with a high thermal expansion coefficient (i.e. $0.89*10^{-3}$ K^{-1}) and due to its low melting point (≈60°C) it becomes adhesive applying heat during lamination, sticking strongly to the receiving material. The formation of wrinkles occurs to minimize the total potential energy of the skin layer and the substrate induced by thermal expansion. The strategy for the realization of the heat-driven wrinkle patterns is illustrated in Figure 6b; once heated, the paraffin wax upon cooling to room temperature, generates a compressive stress at the interface of the bilayer sample, owing to the considerable mismatch between the modulus and thermal expansion ratio of the substrate and the stiff top layer made of RS or RS/yeast [30]. AFM analysis reported in Figure 6c shows that a smooth surface converts into wrinkled state through heating and then cooling down to room temperature.

Preprints (www.preprints.org) | NOT PEER-REVIEWED | Posted: 20 June 2018 doi:10.20944/preprints201806.0320.v1

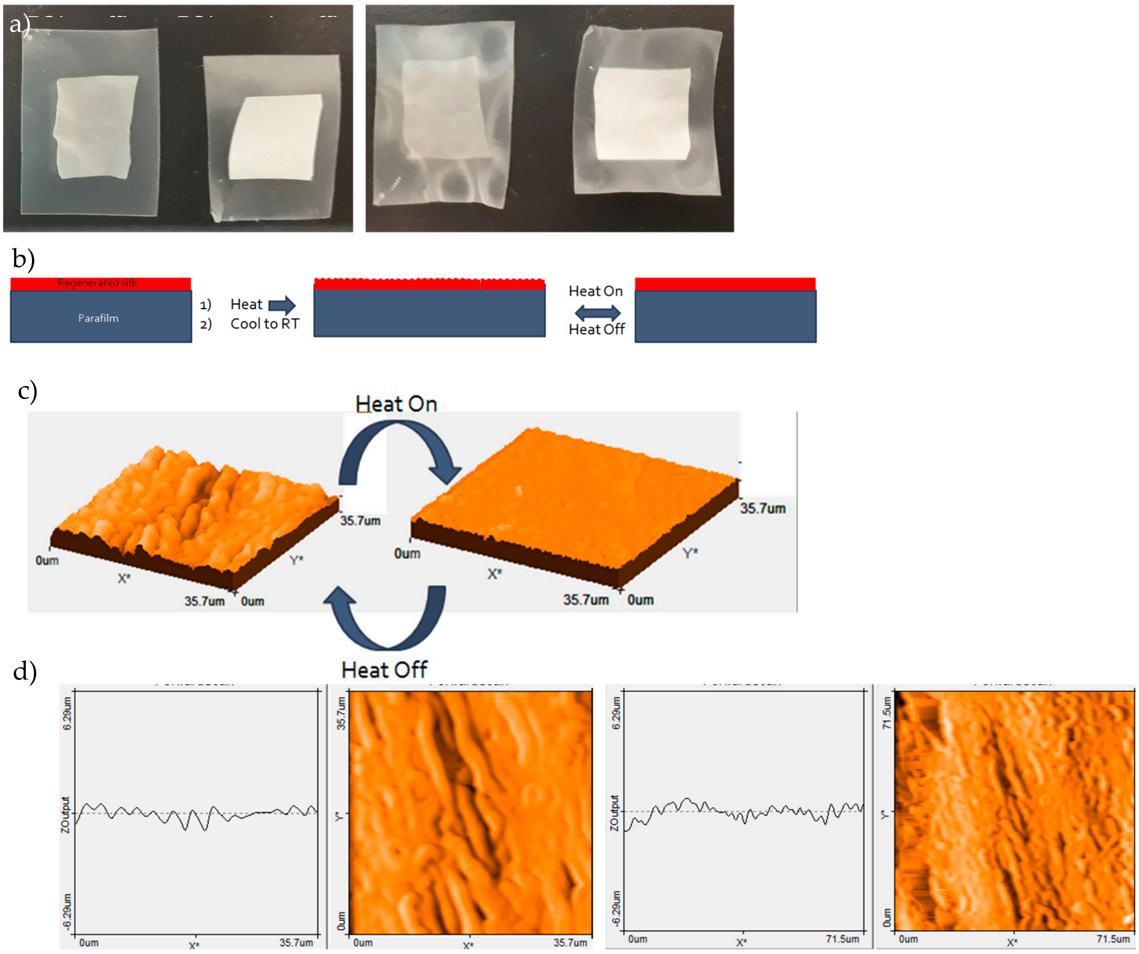

Figure 6. (a) Photographs of RS/yeast/paraffin and RS/paraffin bilayer systems before (left) and after (right) the wrinkle activation. (b) Schematic illustration of temperature driven wrinkling. The bilayer system is flat at room temperature, the heat induces the temperature increasing and thus the thermal expansion of the paraffin substrate, resulting in the increase in the compressive strain of the bilayer systems once cooled down to room temperature with the appearance of the wrinkles. Once the wrinkled state was activated, the heat/temperature can again induce the thermal expansion of the paraffin substrate, resulting in the reversibility of the tempertature-driven wrinkles. (c) AFM images showing the reversibility of the temperature-driven wrinkles. (d) AFM images and related profile images of RS (left) and RS/yeast (right) film layers.

The amplitude (A) and the wavelength (λ) of the wrinkles depend on the thickness and mechanical properties of the skin layer and the substrate and according to linear bucking theory [31-35] can be expressed as:

$$A=h_f((\sigma_0-\sigma_c)/\sigma_c)^{1/2}/a \qquad (1)$$

and

$$\lambda=4.36h_f(E_f(1-\nu_s^2)/(E_s(1-\nu_f^2)))^{1/3}-2A(1-a)/a \qquad (2)$$

where σ_c refers to the critical strain to wrinkle formation and is given as[33]

$$\sigma_c=(1/4)(E_f')^{1/3}(E_s')^{2/3} \qquad (3)$$

and σ_0 is the compressive stress of the film layer at temperature below the heating temperature given by the equation 4 [37]:

$$\sigma_0=(E_f(\alpha_s-\alpha_f)\Delta T)/(1-\nu_f) \qquad (4)$$

 doi:10.20944/preprints201806.0320.v1

where $E'=E/(1-\nu^2)$ and subscript f and s refer to the film layer and the substrate of the bilayer system and E', E and ν are in plane modulus, Young's modulus and Poisson's ratio, respectively. h_f (equal to 1μm) is the film thickness and $0 \leq a \leq 1$ is an adhesion parameter that we have introduced (ideally a=1) for accounting the nonideal bonding between film and substrate (imposing the film inextensibility and simply assuming squared shape wrinkles, i.e. $2A+\lambda$=cost). The Young's modulus for RS, RS/yeast and paraffin are 54 MPa, 37 MPa, 1.4 MPa [18], respectively, and $\nu_f=0.5$. The applied strain ε when the bilayer system is heated is calculated as $\varepsilon=(\alpha_s-\alpha_f)*\Delta T$ where α_s and α_f are the thermal expansion coefficients with $\alpha_s >> \alpha_f$. Finally, the theoretical wavelength and amplitude values obtained from Eq. 1 and Eq. 2 are reported in Tab. 2 and compared with the experimental findings by fitting the single parameter a.

Table 2. Theoretical and experimental (estimated by AFM images and related profiles reported in Fig. 6d) amplitude and wavelength of the different skin layers, with a=0.4.

Sample	$A_{Theor.}$ (μm)	$\lambda_{Theor.}$ (μm)	$A_{Exp.}$ (μm)	$\lambda_{Exp.}$ (μm)
RS/paraffin	2.72	1.83	1.23	2.93
RS/yeast/paraffin	2.20	2.21	1.04	2.14

5. Conclusions

Here we described how incorporating microorganisms in bio-based structural proteins, by providing an opportune nutrient for their growth, can results in a composite material with novel properties. We observed that the fermentation of yeast cells activated in the dissolution bath of silk fibers is critical in determining the β-sheet content of RS and thus the mechanical properties. In particulat the yeast fermentation increases the crystalline content of regenerated silk fibroin, such bionic coating reduces the water permeability and acts as an effective gas barrier, e.g. to increase the shelf-life of perishable food. Then we reported a method which consists of transfer printing the prepared freestanding RS and Rs/yeast layer films onto on self-adherent Parafilm substrate. It is reported how the mechanical characteristics of the film layers as well as the high thermal expansion coefficient of the paraffin substrate can be used to fabricate a sensor with the surface morphology that changes between the wrinkled state and the wrinkle-free state under an external thermal stimulus. This naturally derived material is thus a promising solution for different problems, e.g. a valid alternative for efficient and smart food packaging with respect to traditional polymer-based coatings. Finally, the proposed model can help in the real thus nonideal design of such coatings and the degree of adhesion also emerges as designing parameter for tuning the wrinkle morphologies.

Supplementary Materials: The following are available online, Figure S1: Evolution of the CO_2 absorption peak over period of 7 days for (left) RS/yeast and (right) RS coating, respectively; Figure S2: Water soaked sponges with different types of coatings.

Author Contributions: Conceptualization, L.V. and N.M.P.; Methodology, L.V.; Investigation, S.B.B.; Data Curation, S.B.B.; Writing-Original Draft Preparation, L.V. and N.M.P.; Writing-Review & Editing, L.V. and N.M.P.

Funding: N.M.P. is supported by the European Commission under the Graphene Flagship Core 2 grant No. 785219 (WP14 "Polymer Composites") and FET Proactive "Neurofibres" grant No. 732344 as well as by the Italian Ministry of Education, University and Research (MIUR) under the "Departments of Excellence" grant L.232/2016. L.V. is supported by the Italian Ministry of Education, University and Research (MIUR) under the "Departments of Excellence" grant L.232/2016.

Acknowledgments: Prof. Miguel-Angle Lopez-Manchado (Instituto de Ciencia y Tecnología de Polímeros, ICTP-CSIC, Madrid) is kindly acknowledged for the XRD analysis.

Conflicts of Interest: The authors declare no conflict of interest.

References

1. Cleveland, J.; Montville, T. J.; Nes I. F.; Chikindas, M. L. Bacteriocins: safe, natural antimicrobials for food preservation. *Int. J. Food Microbiol.* **2001**, *71*, 1–20.
2. Paul Ross, R.; Morgan S.; Hill, C. Preservation and fermentation: past, present and future. *Int. J. Food Microbiol.* **2002**, *79*, 3–16.
3. Synowiecki J.; Al-Khateeb, N. A. Production, properties, and some new applications of chitin and its derivatives. *Crit. Rev. Food Sci. Nutr.* **2003**, *43*, 145–171.
4. Ohzono, T.; Monobe, H.; Yamaguchi, R.; Shimizu, Y.; Yokoyama, H. Dynamics of surface memory effect in liquid crystal alignment on reconfigurable microwrinkles. *Appl. Phys. Lett.* **2009**, *95*, 14101.
5. Kim, P.; Hu, Y.; Alvarenga, J.; Kolle, M.; Suo, Z.; Aizenberg, J. Rational Design of Mechano-Responsive Optical Materials by Fine Tuning the Evolution of Strain-Dependent Wrinkling Patterns. *Adv. Opt. Mater.* **2013**, *1*, 381 – 388.
6. Bowden, N.; Huck, W. T. S.; Paul, K. E.; Whitesides, G. M. The controlled formation of ordered, sinusoidal structures by plasma oxidation of an elastomeric polymer. *Appl. Phys. Lett.* **1999**, *75*, 2557 – 2559.
7. Ohzono, T.; Suzuki, K.; Yamaguchi, T.; Fukuda, N. Tunable optical diffuser based on deformable wrinkles. *Adv. Opt. Mater.* **2013**, *1*, 374 – 380.
8. Kim, D. H.; Viventi, J.; Amsden, J. J.; Xiao, J.; Vigeland, L.; Kim, Y. S.; Blanco, J. A.; Panilaitis, B.; Frechette, E. S.; Contreras, D.; Kaplan, D. L.; Omenetto, F. G.; Huang, Y.; Hwang, K. C.; Zakin, M. R.; Litt B.; Rogers, J. A. Dissolvable films of silk fibroin for ultrathin conformal bio-integrated electronics. *Nature Materials* **2010**, *9*, 511–517.
9. Tao, H.; Brenckle, M. A.; Yang, M.; Zhang, J.; Liu, M.; Siebert, S. M.; Averitt, R. D.; Mannoor, M. S.; McAlpine, M. C.; Rogers, J. A.; Kaplan D. L.; Omenetto, F. G. Silk-based conformal, adhesive, edible food sensors. *Advanced Materials* **2012**, *24*, 1067–1072.
10. Marelli, B.; Brenckle, M. A.; Kaplan D. L.; Omenetto, F. G. Silk fibroin as edible coating for perishable food preservation. *Sci. Rep.* **2016**, *6*, 25263.
11. Lawrence, B. D.; Pan, Z.; Liu, A.; Kaplan D. L.; Rosenblatt, M. I. Human corneal limbal epithelial cell response to varying silk film geometric topography in vitro. *Acta Biomaterialia* **2012**, *8*, 3732–3743.
12. Lawrence, B. D.; Marchant, J. K.; Pindrus, M. A.; Omenetto F. G.; Kaplan, D. L. Silk film biomaterials for cornea tissue engineering. *Biomaterials* **2009**, *30*, 1299–1308.
13. Lawrence, B. D.; Wharram, S.; Kluge, J. A.; Leisk, G. G.; Omenetto, F. G.; Rosenblatt, M. L.; Kaplan, D. L. Effect of hydration on silk film material properties. *Macromolecular Bioscience* **2010**, *10*, 393–403.
14. Brenckle, A. M.; Kaplan, D. L.; Omenetto, F. G. Direct Transfer Printing of Water Hydrolyzable Metals onto Silk Fibroin Substrates through Thermal-Reflow-Based Adhesion. *Adv. Mater. Interfaces* **2016**, *3*, 1600094.
15. Jay, S. C. The cocoon of the honey bee, Apis mellifera. *Can. Entomol.* **1964**, *96*, 784–792.
16. Hepburn, H. R.; Kurstjens, S. P. The combs of honeybees as composite materials. *Apidologie* **1988**, *19*, 25–36.
17. Dorset, D. L. The crystal structure of waxes. *Acta Crystallogr. B* **1995**, *51*, 1021–1028.
18. Valentini, L.; Bittolo Bon, S.; Lopez-Manchado, M.-A.; Mussolin, L.; Pugno, N. Development of conductive paraffin/graphene films laminated on fluoroelastomers with high strain recovery and anti-corrosive properties. *Composites Science and Technology* **2017**, *149*, 254-261.

 doi:10.20944/preprints201806.0320.v1

19. Valentini, L.; Bittolo Bon, S.; Signetti, S.; Tripathi, M.; Iacob, E.; Pugno, N. M. Fermentation based carbon nanotube multifunctional bionic composites. *Sci. Rep.* **2016**, *6*, 27031.
20. Ling, S.; Zhang, Q.; Kaplan, D. L.; Omenetto, F.; Buehler, M. J.; Qin, Z. Printing of stretchable silk membranes for strain measurements. *Lab Chip* **2016**, *16*, 2459-2466.
21. Hu, X.; Kaplan D.; Cebe, P. Determining Beta-Sheet Crystallinity in Fibrous Proteins by Thermal Analysis and Infrared Spectroscopy. *Macromolecules* **2006**, *39*, 6161-6170.
22. Q. Lu, X. Hu, X. Wang, J. A. Kluge, S. Lu, P. Cebe and D. L. Kaplan, Water-insoluble silk films with silk I structure. *Acta Biomaterialia* **2010**, *6*, 1380–1387.
23. J. P. Anderson, Morphology and crystal structure of a recombinant silk-like molecule, SLP4. *Biopolymers* **1998**, *45*, 307–321.
24. J. Warringer, E. Ericson, L. Fernandez, O. Nerman and A. Blomberg, High-resolution yeast phenomics resolves different physiological features in the saline response. *PNAS* **2003**, *100*, 15724–15729.
25. L. Valentini, S. Bittolo Bon, S. Signetti and N. M. Pugno, Graphene-Based Bionic Composites with Multifunctional and Repairing Properties. *ACS Applied Materials & Interfaces* **2016**, *8*, 7607-7612.
26. A. Seidel, O. Liivak, S. Calve, J Adaska, G. Ji, Z. Yang, D. Grubb, D. B. Zax and L. W. Jelinski, Regenerated Spider Silk: Processing, Properties, and Structure. *Macromolecules* **2000**, *33*, 775-780.
27. K. Van de Velde, P. Kiekens, Biopolymers: overview of several properties and consequences on their applications. *Polym. Test.* **2002**, *21*, 433–442.
28. D. S. Im, M. H. Kim, Y. I. Yoon, W. H. Park. Gelation behaviors and mechanism of silk fibroin according to the addition of nitrate salts. *Int. J. Mol. Sci.* **2016**, *17*, 1697.
29. A. Matsumoto, J. Chen, A. L. Collette, U. J. Kim, G. H. Altman, P. Cebe and D. L. Kaplan, Mechanisms of silk fibroin sol-gel transitions. *J. Phys. Chem. B* **2006**, *110*, 21630 – 21638.
30. Hou, H.; Yin, J.; Jiang, X. Reversible diels-alder reaction to control wrinkle patterns: from dynamic chemistry to dynamic patterns. *Adv. Mater.* **2016**, *28*, 9126 – 9132.
31. Rodríguez-Hernández, J. Wrinkled interfaces: taking advantage of surface instabilities to pattern polymer surfaces. *Prog. Polym. Sci.* **2015**, *42*, 1 – 41.
32. Chen, C.-M.; Yang, S. Wrinkling instability in polymer films and their applications. *Polym. Int.* **2012**, *61*, 1041 – 1047.
33. N. Bowden, S. Brittain, A. G. Evans, J. W. Hutchinson, G. M. Whitesides, Spontaneous formation of ordered structures in thin films of metals supported on an elastomeric polymer. *Nature* **1998**, *393*, 146 – 149.
34. C. M. Stafford, C. Harrison, K. L. Beers, A. Karim, E. J. Amis, M. R. VanLandingham, H.-C. Kim, W. Volksen, R. D. Miller, E. E. Simonyi, A buckling-based metrology for measuring the elastic moduli of polymeric thin films. *Nat. Mater.* **2004**, *3*, 545 – 550.
35. Wang, Q.; Zhao, X.; Beyond wrinkles: Multimodal surface instabilities for multifunctional patterning. *MRS Bull.* **2016**, *41*, 115 – 122.
36. Allen, H. G. Analysis and Design of Structural Sandwich Panels (Pergamon, New York, 1969).
37. Ohring, M. The Material Science of Thin Films (Academic, San Diego, 1992).